
Proceedings Paper:
Mitchinson, B., Pearson, M., Melhuish, C. et al. (2006) A model of sensorimotor coordination in the rat whisker system. In: Nolfi, S., Baldassarre, G., Calabretta, R., Hallam, J.C.T., Marocco, D., Meyer, J.A., Miglino, O. and Parisi, D., (eds.) From Animals to Animats 9. 9th International Conference on Simulation of Adaptive Behavior, SAB 2006, September 25-29, 2006, Rome, Italy. Springer-Verlag , Berlin Heidelberg, pp. 77-88. ISSN: 0302-9743.

https://doi.org/10.1007/11840541

A Model of Sensorimotor Coordination in the Rat Whisker System

Ben Mitchinson[1], Martin Pearson[2], Chris Melhuish[2], Tony J. Prescott[1]

[1] The University of Sheffield t.j.prescott@shef.ac.uk
[2] The University of the West of England

Abstract. The rat has a sophisticated tactile sensory system centred around the facial whiskers. During normal behaviour, rats sweep their longer whiskers (macrovibrissae) through the environment to obtain large-scale information, whilst gathering small-scale information with the sensory apparatus around their snout. The macrovibrissae are actively and differentially controlled. Using high-speed video recording, we have observed that temporal and spatial parameters of whisking pattern generation are modulated to match environmental features such as the position and orientation of nearby surfaces. Whisking is also closely co-ordinated with head and body movements, allowing the animal to locate and orient to interesting stimuli detected through whisker contact. In this paper, we present a hybrid (spiking-neuron/arithmetic) model of the neural systems underlying these observed adaptive sensorimotor behaviours, and demonstrate its performance in a simulated robot with rat-like morphology. We also report progress towards embedding these control systems in a physical robot with biomimetic whiskers.

1 Introduction

The rat possesses an impressively acute tactile sensory system, the sensors of which include large mobile whiskers on either side of the snout [1]. Tactile information is gathered by sweeping these whiskers forwards and backwards at 5-25 Hz, and there is now strong evidence that this behavior is generated by output from a 'whisking pattern generator' (WPG) located in the rat hindbrain [2]. Interestingly, the parameters of whisking appear to be controlled independently on each side of the snout in response to changes in the environment and/or the motivation of the animal [3–6], presumably to optimise perception. Furthermore, studies have long shown that rodents orient their snout towards novel stimuli, apparently to bring more rostral sensory apparatus (small immobile whiskers, teeth, tongue, lips and nose) to bear on items of possible interest. Computational modelling of these aspects of sensorimotor co-ordination in the rat's tactile perception system is the focus of this study.

Using high-speed video recording [7] we have observed patterns of asymmetrical contact with walls and objects suggesting that rats regulate their whisker movements so as to control the nature of these contacts. Specifically, the whiskers appear to be actively moved forwards to meet more rostral objects ('maximal

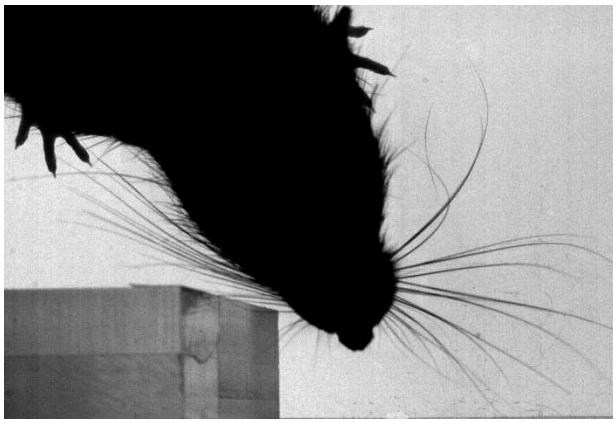

Fig. 1. Still from high-speed video of genetically-blind rat encountering obstacle unilaterally. Ipsi-/contra-lateral whiskers are retracted/protracted in response.

contact'), and, at the same time, actively restrained from pushing unduly against more caudal objects ('minimal impingement'). This control strategy is intuitively satisfying as it would tend to maximize the number of contact/detach events between the whiskers and the environment that have been found to lead to robust sensory responses (known as 'ON' and 'OFF' responses) in the primary afferent nerves [8]. Whilst maximizing the rate of information collection, this scheme would also minimize the distortion that could arise through overdriving the sensory apparatus (since the whisker deflections generated by such events will tend to be small). This interpretation is consistent with previous observations of rat whisking behaviour (though see [4, 5] for further discussion).

The minimal impingement element of this hypothesized control strategy can be implemented through negative feedback that inhibits protraction (forward motion) of the whiskers when contact occurs. Direct projections from trigeminal sensory nuclei to the facial motor nucleus, both located in the hindbrain, have been identified [9, 10] that could provide a substrate for negative feedback in the form of a simple, closed sensorimotor loop (see [11] for further functional anatomical information). Maximal contact, on the other hand, requires knowledge of something located outside the range of the normal whisker sweep. In the genetically blind animals that we study it is thus only observed in response to contact events from earlier whisks, or to contact events on the opposite side of the snout (see [12] for evidence of increased protraction given prior knowledge of rostrally-located items). The pose depicted in Figure 1 is typical, with the whiskers ipsilateral to an obstacle swept back, and those contralateral swept forward. Memory for past sensory events most likely requires cortical pathways, therefore, whilst hindbrain, contralateral positive feedback could provide the substrate for a reactive maximal contact control pathway, some cortical modulation of the WPG is presumably required when memory is involved. In the current study we therefore investigate direct, contralateral positive feedback only.

Accurate orienting of the head/snout to a point of whisker contact requires more advanced circuitry than that proposed for hindbrain feedback control. The midbrain superior colliculus (SC) is known to be essential for the expression of orienting responses to somatosensory stimuli [13], and projections from trigeminal sensory neurons to SC have been identified repeatedly, e.g. [14]. We chose, therefore, to model a sensorimotor loop through SC to mediate orienting. SC is known to use a retino-centric coordinate system, which we approximate as head-centric – what remains, then, is to specify the nature of the transform from the whisker-centric encoding in trigeminal to a head-centric reference frame. Two strategies for instantiating this transformation have been proposed: temporal decoding using neuronal phase-locked loops, and spatial decoding, through the integration of information from contact receptors with that from whisking angle/phase receptors [15]. We chose the latter, for its simplicity.

Below, we present a simulated mechanical environment ('WhiskerWorld') which we use for testing our control models. We also outline our earlier model of whisker sensory transduction [16] which is used to generate biologically accurate spiking input signals for the new models studied here (Section 2). We then detail a hybrid (spiking/non-spiking) computational simulation model of the above aspects of active perception in rat (Section 3), and illustrate its performance in WhiskerWorld (Section 4). We conclude by outlining the proposed embodiment of these computational features in a mobile robot (Section 5).

2 Simulated Environment

Our model environment consists of a two-dimensional simulation of mechanical interactions between six inflexible whiskers and assorted circular obstacles (Figure 7). The whiskers are carried three on each side of the snout of a simulated robot platform with complete freedom of mobility in the plane. The positions of the whisker bases are computed from the location of the platform and its neck angle. For each whisker we also specify its length, the more rostral whiskers being shorter, and the positive acute angle it makes with the symmetry axis of the head, $\theta_{1...6}$. One simulated muscle drives each row of whiskers to protract (there is evidence of row-based motor circuits in the rat [17]), whilst intrinisic elastic forces drive them to retract [3]. Interactions with the immobile elastic obstacles also drive the whiskers as appropriate. Whiskers that temporarily intersect obstacles are considered 'deflected', to a degree and direction, x, concomitant with the intersection and its location along the whisker. The control loops to be discussed (a) drive the simulated protraction muscles such that maximal contact and minimal impingement are elicited, and (b) drive the wheels and neck of the mobile platform such that the robot's 'foveal zone' (indicated in Figure 7) is brought to bear on obstacles in a biologically convincing movement.

When a model whisker makes contact with an object the resulting deflection x is input to a simulation of the mechanical properties of the rat whisker follicle [16]. The output of this mechanical model is used to generate spike trains in model sensory neurons whose response properties were derived from an ex-

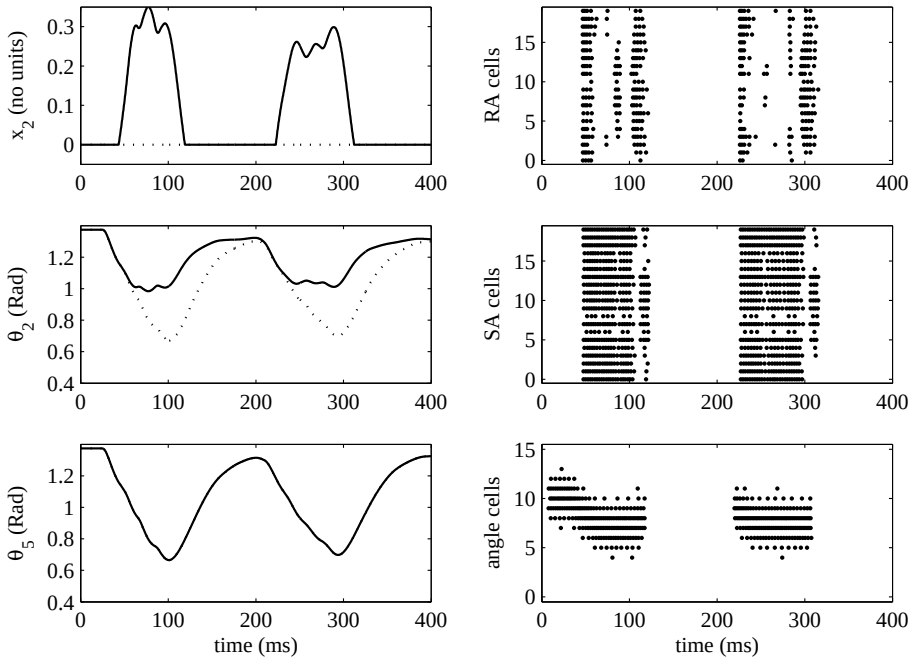

Fig. 2. Two whisks with a unilateral whisker-field obstruction recorded in WhiskerWorld with no sensorimotor feedback. θ_2 is the angle of the obstructed whisker, θ_5 the angle of the corresponding unobstructed whisker on the other side of the snout; with an obstacle present (solid) and without (dotted). x_2 is the deflection of the obstructed whisker. Right-hand panels show responses of SA, RA, and angle neurons to the obstructed whisks, where each dot represents a spike.

tensive review of relevant electrophysiological studies. Each simulated whisker drives 20 'slowly-adapting' (SA) and 20 'rapidly-adapting' (RA) neurons that together encode the deflection of the whisker. Additionally, 16 model neurons encode the whisker angle θ in analogy to the 'angle/phase' afferents recently discovered in the rat [15]. During a typical obstructed (and unmodulated) whisk, θ decreases (with protraction) until contact occurs, θ is then arrested whilst x displays a pulse resulting from the deflection of the whisker against the obstacle, finally the whisker detaches from the obstacle and θ increases as it falls back to its rest position. This sequence is illustrated in the left panels of Figure 2. In the right panels of that figure are shown typical responses of model sensory neurons to the signals on the left. The RA cells are all similar (save for some structural noise) except each responds most strongly to a different direction of whisker deflection. The neuron with index 0 is tuned to deflection in the positive x direction, and the remainder are uniformly spaced around the circle in x/y (although we do not simulate deflections in the y direction, that is, into the simulated plane, here). The cells that respond most strongly to a positive x

deflection (around index 0) spike one to five times in response to contact (the ON response); those that respond most strongly to negative x deflection (around index 10) respond similarly to detach (the OFF response). However, all RA cells in this example express ON and OFF responses to the substantial deflection signals. The response of the SA cells is similar, except that they show continued responses (with firing rates as high as 400Hz) throughout the deflection period. The angle cells encode θ in a distributed way: the cells have preferred values of θ linearly related to their index, and respond more strongly as θ approaches this value. The cells used here do not respond at all during retraction (as was found for a majority of angle/phase cells in [15]).

3 Simulated Control Loop Models

3.1 Whisking Pattern Generator and Pattern Modulation

The core of the whisking pattern generator (WPG) is a self-resetting integrator (Figure 3) built from two spiking neuron populations. Activity in an 'integrator' population builds up spontaneously over time, then, at some threshold, excitatory drive from these cells to a 'reset' population causes the latter to become active; the integrator neurons are quickly silenced by inhibition from the reset population; activity in the reset population then dies away, and the cycle begins again. This core generator, which runs at around 5Hz in all simulations, provides excitation to two 'output-buffer' populations of spiking cells that are subject to diffuse modulation from all SA cells and are thus the site of modulation by sensory signals. Specifically, the SAs provide ipsilateral inhibition and contralateral excitation to output-buffer neurons, implementing, respectively, the required negative and positive feedback. As implemented, this modulation is linear, so excitation tends to raise the set-point of the output activity whilst inhibition tends to reduce and delay output activity (see insets in figure). Activity in each output population is converted to a scalar rate by driving a leaky integrator (time constant 10ms) with the sum of all cell spikes. The resulting two signals are then used as muscle drive forces in the physical simulation. Note that whilst the pattern generators for the two sides are coupled in phase throughout, the whisk patterns they generate are able to differ in set-point and amplitude.

3.2 Coincidence Detector and Orienting Behaviour

The coincidence detector (CD) consists of 6 banks of 16 spiking cells each, with the mth cell in the nth bank receiving excitation from all RA cells and from the mth angle cell associated with the nth whisker. Since we do not deal with deflections out of the simulation plane in the current model, there is no need to distinguish which RA cells from the whisker were stimulated. This connectivity is sufficient to perform coincidence detection, but is not robust against noisy inputs, generating both false positives and false negatives. The addition of strong surround inhibitory connections within each cell bank greatly improves noise

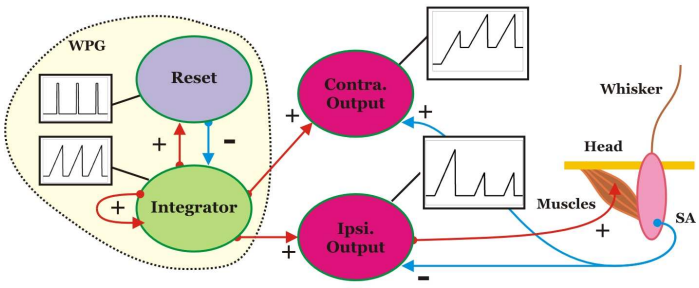

Fig. 3. (Left) Core generator consists of two reciprocally connected cell populations ('integrator' and 'reset'). (Right) Output populations driven by core generator also accept modulation from sensory afferents (SAs). Each population consists of 40 cells.

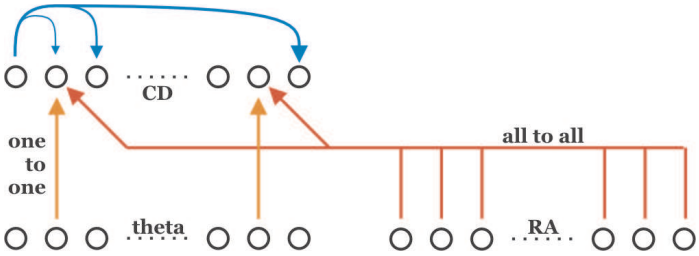

Fig. 4. Summary of connectivity between one whisker follicle and one bank of the coincidence detector. Red represents excitatory afferents, whilst blue represents recurrent surround inhibition, with strength related to separation in θ.

resistance. Specifically, we used inhibition with relative strength given by the inverted Gaussian function $w = \exp((\theta_i - \theta_j)^2/\Delta\theta^2)$, with $\theta_{i,j}$ the preferred angles of connected cells, and $\Delta\theta$ a parameter. The connectivity of one bank is illustrated in Figure 4.

The CD operates as follows. Activity in the RA cells serving the nth whisker coincident with activity in the angle cells serving the nth whisker and tuned to around $\theta = \theta_0$, results in activity in the nth bank of the CD, in the cells corresponding to those angle cells. This activity rapidly and effectively silences sub-threshold activity in other cells in the bank, leaving a well-defined locus of activity in one or a few cells. The identity of these active cells encodes the location at which a whisker contacted the environment in a head-centric coordinate frame. The direction of whisker-sweep (forwards/backwards) is encoded by the identity of the cells within a bank, and in the transverse direction (left/right) by the identity of the bank, though the latter is encoded more indirectly since there is no guarantee that contact occurred at the whisker tip, or that multiple whiskers will not encounter the same or different obstacles. Having implemented a transform from whisker-centric to head-centric contact data, it is straightforward, then, to assign each of the 96 cells in the CD to a region in the simulation plane, relative

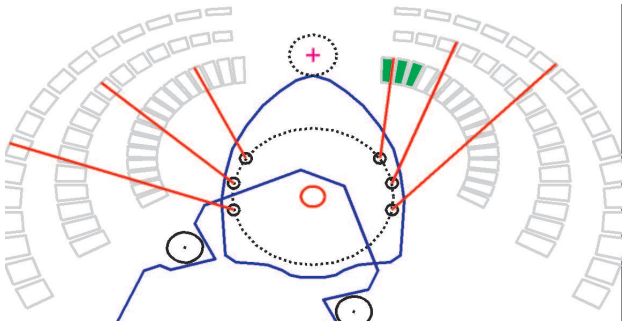

Fig. 5. Typical contact regions for each cell in the CD mapped on to a head-centric coordinate system. Active (filled) regions represent activity recorded concurrently with the last panel of Figure 7.

to the head, wherein contact will typically lead to activity in that cell. These locations are illustrated in the head-centric representation of Figure 5.

Orienting itself is implemented arithmetically. Around the point of maximum protraction, the reset population of the WPG pulses briefly. If any single CD cell has over-threshold activity at that time, an average is taken across the assigned locations of each over-threshold cell, and that location is deemed 'interesting'. A path-following algorithm then moves the neck and wheels of the mobile platform such that the foveal zone of the robot follows a direct path to the interesting location, using the neck as much as possible, and moving the wheels only as much as necessary. This algorithm is satisfying, firstly because the calculations are simple (neck follows nose, tail follows neck) and secondly because animals display this 'recruitment' of joints as a movement progresses [18]. Forcing the foveal point to follow a path that loops backwards somewhat (to form a slight 'U') is an alternative strategy that might reduce the incidence of collisions.

4 Performance of the Simulated Model

We repeated the simulation reported in Figure 2, incorporating feedback modulation of the WPG (see Figure 6). The effect of the modulation on the whisking range of whisker 2 (ipsilateral) can be seen as it works more towards the back of the head (θ_2 increases). Furthermore, the protraction force applied to the ipsilateral whiskers ceases soon after contact occurs, so that both contacts are briefer and cleaner than those returned without feedback. The RA cells for whisker 2 now clearly show ON and OFF responses, and nothing else – the spurious additional responses seen in Figure 2 are absent. The SA cells show a much briefer response than before, as a result of the briefer contact – their overall response profile is thus quite similar to that of the RA cells. The response of the angle cells is largely unchanged. The contralateral whiskers (represented here by whisker 5) are swept substantially further forward than in the unobstructed reference plot (θ_5 decreases), illustrating the effect of the contralateral positive feedback. The

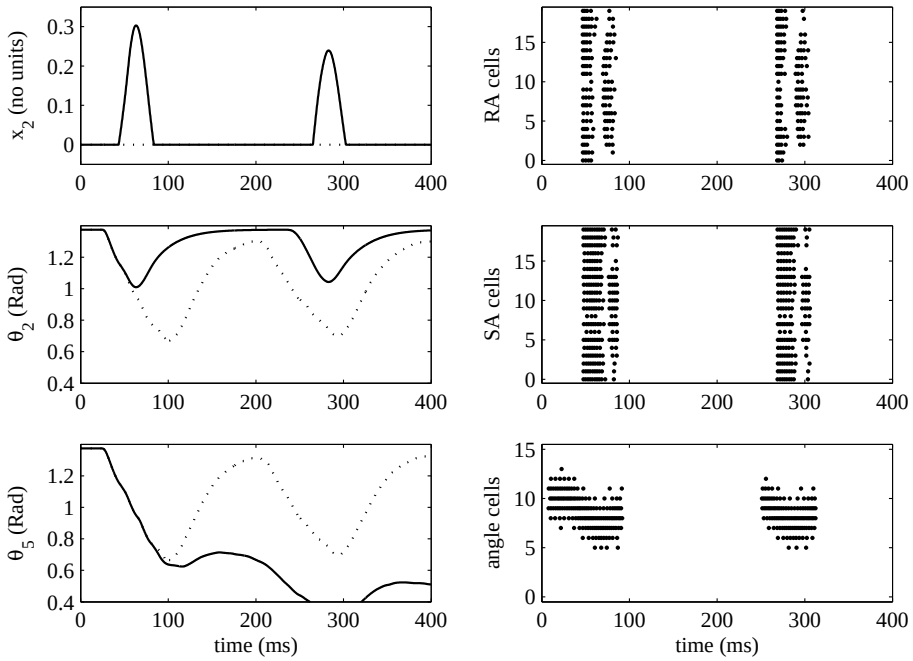

Fig. 6. Two whisks with unilateral whisker-field obstruction recorded in WhiskerWorld *with* sensorimotor feedback. Panels are exactly as for Figure 2.

contralateral whisk amplitude is also reduced, since the mechanical advantage of the muscles is less at this whisking angle – see [3] for a fuller description of the whisking mechanics on which our simulation is based, along with the analogous biological result of amplitude reduction during forward-swept whisking.

Next, we repeated the same simulation, incorporating the CD and orienting response. Soon after contact with the obstacle, the simulated robot 'foveates' to the point of contact, as shown in Figure 7. At $t = 0$, the robot is in its initial state. At $t = 65ms$, the ipsilateral output population of the WPG has been silenced by negative feedback and the ipsilateral whiskers have reached peak protraction. At $t = 110ms$, orienting has just begun with a neck movement; the movement is still almost entirely of the neck until $t = 165ms$ when the body begins to be recruited. At $t = 300ms$ the orienting movement is complete, the second whisk is at around full protraction, and the forward-most contralateral whisker contacts the obstacle, thus illustrating the functional justification for their forward sweep. Note that the orient is specifically to the point of contact, rather than to the nearest face of the obstacle (say). This illustrates both the high resolution of the system despite the paucity of cells involved, and that this whisker sensory system detects surfaces rather than objects. The performance of the WPG and afferents during this orienting movement is similar to that shown in Figure 6, except that the second contact occurs on a different whisker.

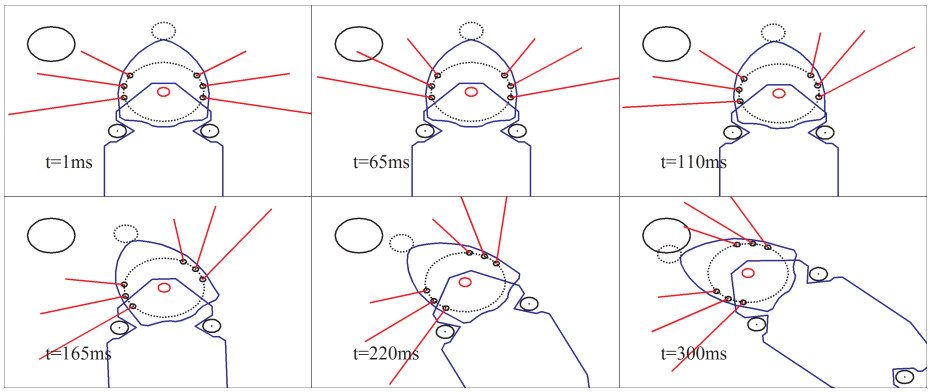

Fig. 7. Simulated evironment: non-interacting robot platform carries six whiskers which interact mechanically with environmental obstacles; dotted circle in front of snout indicates 'foveal zone'. Each panel represents the situation at the time shown during an orient-to-stimulus behaviour.

5 Towards a Robot Implementation

The control models detailed above will soon be implemented on a mobile robot platform so that we can investigate their performance in a noisy real-world environment. The physical platform will have a mechanical architecture as shown in Figure 7 (the simulation is modelled on the robot design), driven by two of three omni-directional wheels and with a driven neck joint, and is intended to coarsely reflect the morphology of the rat. The six artificial whiskers are of moulded glass fibre, 100-200mm long, and weigh around half a gram. Additional whisker rows can be stacked vertically in the future to more closely emulate the array of vibrissae of the rat mystacial pad. All whiskers share the same taper profile, so the base diameter (1-2mm) is proportional to the length. At the base of each whisker, four strain gauges are mounted longitudinally at ninety-degree intervals, and wired into 2 half-bridge configurations. Each opposing pair measure the strain in opposite faces of the whisker, so that the bridge outputs are monotonic (almost linear) with the deflection of the whisker in each dimension (x, studied in simulation above, and y, up and down). This transduction configuration has proven to have very low noise (better than 60dB SNR) and is extremely sensitive to mechanical deflections in the whisker shaft at any point along its length. The whiskers are driven using a biomimetic system of 'shape metal alloy' wire (BioMetal©) to provide a protraction force analogous to that of muscles, with retraction driven by a spring analogous to the elasticity of the facial tissues. θ is measured directly using an optical quadrature shaft encoder mounted onto the whisker spindle. Full details of the whiskers and whisker drive mechanism (Figure 8) are given in [19]. The x/y deflection signals are passed to the follicle model [16]: a reduced form of the mechanical part of this model is embedded in a DSP processor, whilst nearly 400 primary afferent models are embedded us-

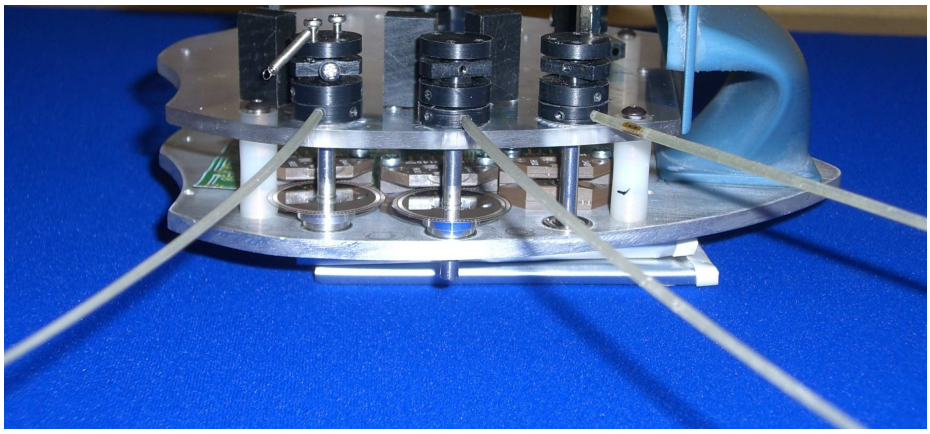

Fig. 8. Photograph of the robot head showing base of whiskers, mounted gauges, 'follicle' spindles with angle encoders, and biowire drive mechanism (STAND-IN PHOTO).

ing a custom built FPGA module, employing a pipelined parallel computation architecture to achieve real time perfomance. The output from this, a wide bus of individual bit streams carrying the spike/no-spike state of each afferent, is distributed to an array of further FPGA modules housing the models discussed above. This neural processing system will share space onboard the robot with an x86-based PC, which will house the remainder of the software system. The PC will also log software and hardware states during short experiments – in this way we hope to perform 'virtual electrophysiology' on the robot, realising previously reported biological experiments *in silico* for direct comparison.

6 Discussion

We have demonstrated a simple spiking-neuron model of whisking motor pattern generation that incorporates sensorimotor feedback. We have shown that the model adaptively modulates whisking to suit the environment, and we have illustrated how two types of feedback have the potential to improve the performance of the sensory system in gathering information: ipsilateral negative feedback by ensuring clean stereotypical contacts, contralateral positive feedback by generating contacts that would not otherwise have occurred. The pattern generator presented here is constrained to generate synchronous whisking – whiskers on each side of the snout move in phase – and our model of sensorimotor modulation does not directly affect pattern generation, only its efferent copy. Asynchronous whisking has been previously observed, though only rarely. In our own behavioural work, however, we have formed the impression that asynchrony is frequently triggered by obstacle contact, with synchrony recovering once the rat moves away from the contacted surface. In ongoing work, we are exploring the possibility that loosely-coupled bilateral whisking pattern generators, modu-

lated by sensory input in a similar way to that described above, could reproduce this coupling between asymmetry and asynchrony in an emergent fashion. In the current paper, we have also described a model of orient-to-stimulus behaviour implemented using a mixture of spiking-neuron computation and arithmetic techniques, and have illustrated how this can be used to bring 'foveal' sensors to bear on a whisker contact point. This model required that a whisker-centric to head-centric coordinate transform be applied to the raw sensory data. We have demonstrated how a previously discussed algorithm (detection of activity coincidence between contact and angle afferents) can be implemented for this purpose using a network of spiking neurons. Taken together, these simulations show that sensorimotor coordination alone can explain several major aspects of the observed investigative whisking behaviour of rats.

We have outlined our continuing progress towards the incorporation of these simulated models in the control system of a mobile robot platform. In the future, we will report on the performance of this embedded implementation. There have been several previous artificial whisker implementations [20–23] that have concentrated on what can be achieved functionally with 'bio-inspired' whiskers and whisker arrays, and have shown interesting results in relation to texture and shape discrimination and learning. In most of this existing work the whiskers have been actuated using unmodulated, symmetrical whisking patterns. In contrast, the focus of our research has been to analyse, using high-speed video recording, the 'active whisking' strategies of freely moving rats and to design an artificial system capable of replicating them. In this endeavour, our system aims to remain faithful to the biology wherever possible. In particular, our whiskers are tapered, length-scaled through the row, and measure deflections in two dimensions, and the morphology of the robot/simulation well reflects that of the animal. We have carefully examined signal transduction in the rat whisker follicle, and have designed our artificial transduction system to mimic this. Processing elsewhere in the model architecture is also largely neural, and modeled where possible on identified neural substrates. With this approach, we hope to maintain a direct correspondence between the animal and the engineered system, facilitating knowledge transfer between biology and engineering and vice versa.

References

1. Waite, P.: Trigeminal sensory system. In Paxinos, G., ed.: The Rat Nervous System. Elsevier (2004) 817–851
2. Gao, P., Bermejo, R., Zeigler, H.: Whisker deafferentation and rodent whisking patterns: Behavioral evidence for a central pattern generator. J Neurosci **21** (2001) 5374–5380
3. Berg, R., Kleinfeld, D.: Rhythmic whisking by rat: Retraction as well as protraction of the vibrissae is under active muscular control. J Neurophysiol **89** (2003) 104–117
4. Sachdev, R., Berg, R., Champney, G., Kleinfeld, D., Ebner, F.: Unilateral vibrissa contact: Changes in amplitude but not timing of rhythmic whisking. Somatosens Mot Res **20** (2003) 163–169
5. Hartmann, M., Towal, R.: Bilateral asymmetries in whisking patterns of freely behaving rats. Society for Neuroscience, Washington, Board 625.2 (2005)

6. Mitchinson, B., Prescott, T., Gurney, K., Pearson, M., Gilhespy, I., Pipe, A.: A computational model of a brainstem loop for whisker pattern generation. Society for Neuroscience, Washington, Board 625.4 (2005)
7. Prescott, T., Mitchinson, B., Redgrave, P., Melhuish, C., Dean, P.: Three-dimensional reconstruction of whisking patterns in freely moving rats. Society for Neuroscience, Washington, Board 625.3 (2005)
8. Shoykhet, M., Doherty, D., Simons, D.: Coding of deflection velocity and amplitude by whisker primary afferent neurons: Implications for higher level processing. Somatosens Mot Res **17** (2000) 171–180
9. Pinganaud, G., Bernat, I., Buisseret, P., Buisseret-Delmas, C.: Trigeminal projections to hypoglossal and facial motor nuclei in the rat. J Comp Neurol **415** (1999) 91–104
10. Nguyen, Q., Kleinfeld, D.: Positive feedback in a brainstem tactile sensorimotor loop. Neuron **45** (2005) 447–457
11. Kleinfeld, D., Berg, R., O'Connor, S.: Anatomical loops and their electrical dynamics in relation to whisking by rat. Somatosens Mot Res **16** (1999) 69–88
12. Carvell, G., Simons, D.: Biometric analyses of vibrissal tactile discrimination in the rat. J Neurosci **10** (1990) 2638–2648
13. Di Scala, G., Schmitt, P., Karli, P.: Unilateral injection of GABA agonists in the superior colliculus: Asymmetry to tactile stimulation. Pharmacol Biochem Behav **19** (1983) 281–285
14. Veinante, P., Deschênes, M.: Single- and multi-whisker channels in the ascending projections from the principal trigeminal nucleus in the rat. J Neurosci **19** (1999) 5085–5095
15. Szwed, M., Bagdasarian, K., Ahissar, E.: Encoding of vibrissal active touch. Neuron **40** (2003) 621–630
16. Mitchinson, B., Gurney, K., Redgrave, P., Melhuish, C., Pipe, A., Pearson, M., Gilhespy, I., Prescott, T.: Empirically inspired simulated electro-mechanical model of the rat mystacial follicle-sinus complex. Proc R Soc Lond B Biol Sci **271** (2004) 2509–2516
17. Klein, B., Rhoades, R.: Representation of whisker follicle intrinsic musculature in the facial motor nucleus of the rat. J Comp Neurol **232** (1985) 55–69
18. Dean, P., Redgrave, P., Sahibzada, N., Tsuji, K.: Head and body movements produced by electrical stimulation of superior colliculus in rats: Effects of interruption of crossed tectoreticulospinal pathway. Neuroscience **19** (1986) 367–380
19. Pearson, M., Gilhespy, I., Melhuish, C., Mitchinson, B., Nibouche, M., Pipe, A., Prescott, T.: A biomimetic haptic sensor. Int J Adv Robotic Sy **2** (2005) 335–343
20. Fend, M., Bovet, S., Yokoi, H., Pfeifer, R.: An active artificial whisker array for texture discrimination. In: Proc of the IEEE/RSJ Int Conf on Intelligent Robots and Systems (IROS). (2003) Las Vegas.
21. Kim, D., Möller, R.: A biomimetic whisker for texture discrimination and distance estimation. In: Proc of the Int Conf on the Sim of Adap Behav (SAB). (2004)
22. Seth, A., McKinstry, J., Edelman, G., Krichmar, J.: Texture discrimination by an autonomous mobile brain-based device with whiskers. In: Proc of the IEEE Int Conf on Robotics and Automation (ICRA). (2004)
23. Schultz, A., Solomon, J., Peshkin, M., Hartmann, M.: Multifunctional whisker arrays for distance detection, terrain mapping, and object feature extraction. In: Proc of the IEEE Int Conf on Robotics and Automation (ICRA). (2005)